Biosensors and Bioelectronics 126 (2019) 292–300

Contents lists available at ScienceDirect

Biosensors and Bioelectronics

journal homepage: www.elsevier.com/locate/bios

An impedance biosensor for simultaneous detection of low concentration of *Salmonella serogroups* in poultry and fresh produce samples

Ibrahem Jasim[a], Zhenyu Shen[b], Zahar Mlaji[a], Nuh S. Yuksek[c], Amjed Abdullah[a], Jiayu Liu[a], Shib Ghosch Dastider[d], Majed El-Dweik[e], Shuping Zhang[b], Mahmoud Almasri[a,*]

[a] Department of Electrical and Computer Engineering, University of Missouri, 411 S. 6th St., room 201, Columbia, MO 65211, USA
[b] Department of Veterinary Pathobiology, University of Missouri, Columbia, MO 65211, USA
[c] Globalfoundries, Albany, NY, USA
[d] Cavendish Kinetics, San Francisco, CA, USA
[e] Co-Operative Research and Life Physical Sciences, Lincoln University, Jefferson City, MO 65101, USA

ARTICLE INFO

Keywords:
Dielectrophoresis
Pathogens
Antibodies
Impedance

ABSTRACT

This paper reports the design, fabrication and testing of a microfluidic based impedance biosensor for rapid and simultaneous detection of three *Salmonella* serogroups. The microfluidic device consists of three microchannels, each one includes a region for focusing the *Salmonella* cells into the centerline of the microchannel and direct them toward the sensing region to obtain highly concentrated samples using positive dielectrophoresis force. A region for bacteria sensing consists of interdigitated electrode (IDE) array with 10 pairs of fingers. Three types of *Salmonella* antibodies (type B, D and E) were mixed separately with the cross-linker (Sulfo-LC-SPDP) to enhance the immobalization of the antibodies to the detection electrodes. The electrode surfaces was then functionalized with the three mixtures, one for each channel. As target *antigen* binds to the antibody, it results in impedance change. The *Salmonella* samples were spiked with *Salmonella* type B, introduced into the biosensor via the sample inlet into the focusing region, and then toward the sensing region where they bind to the immobilized antibody, causing a change in the impedance. The performance of the devices was tested using single *Salmonella serotype* B and two *Salmonella* serotypes B, and D, with a limit of detection of 7 cells/ml. The biosensor was also able to differentiate live from dead bacteria eliminating the false positive results. Finally, the device was also able to detect *Salmonella* selectively when other type of pathogen was present.

1. Introduction

Infectious diseases caused by foodborne pathogens such as *Salmonella*, *Listeria*, and *Escherichia coli O157:H7* are the second leading cause of mortality throughout the world after cardiovascular disease (World Health Organization, The World Health Report World Health Organization, Genève, 2004). Annually, millions of infections in the U.S alone are caused by the foodborne pathogens. The estimations of the Centre for Disease Control and Prevention CDC are that 48 million people get sick every year, leading to more than 128,000 hospitalizations and 3000 deaths (Burden of Foodborne Illnesses in the United States, Estimates of Foodborne Illness, CDC). Infections that are caused by *Salmonella* are ranked to be the top among all the foodborne bacterial outbreaks. There were sixteen food related outbreaks in the second half of 2012 in the U.S. *Salmonella* alone is estimated to cause one million human infections each year in the United States resulting in 19,000 hospitalizations and 380 deaths (*Salmonella* Homepage, CDC). Economically, there is a huge cost related to foodborne pathogens due to medical expenses and product recalls (Scallan et al., 2011).

Salmonella enterica are divided into more than 2500 serotypes which are grouped into approximately 50 serogroups (Brenner et al., 2000). *Salmonella* enterica is among the most frequently reported causes of foodborne disease. Infection of *Salmonella* is characterized with the symptoms of diarrhea, abdominal cramps, and fever appearing 6–72 h of eating contaminated food. Patients usually recover within 3–7 days without treatment but infants, the elderly, and immune-compromised persons may develop reactive arthritis, focal infection, and blood infection (McGhie et al., 2009).

The food industry relies on traditional microbiological detection methods, Polymerase Chain Reaction (PCR), and enzyme-linked immunosorbent assay (ELISA) for the detection and identification of foodborne pathogens. The most basic technique is the traditional bacterial

* Corresponding author.
E-mail address: almasrim@missouri.edu (M. Almasri).

https://doi.org/10.1016/j.bios.2018.10.065
Received 26 September 2018; Received in revised form 28 October 2018; Accepted 30 October 2018
Available online 01 November 2018
0956-5663/

culture testing method. Although it's the gold standard testing method it's time consuming and takes 2–5 days to confirm diagnosis (Foodborne Illness and Disease). The PCR technologies offer quantitative, high sensitivity measurements (Sayad et al., 2016). It is popular among the food industry because it reduced the testing time to 24 h plus the shipping time to a testing lab, assuming the company does not own the system. Although the PCR instrument may do the test in 45 min, the need for enrichment step is what makes this testing method requires 24 h. In addition, PCR requires expensive laboratory facilities and equipment, relies on skilled technical expertise, and it may results in false positive due to the presence of inhibitors (Hyeon and Deng, 2017; Zheng et al., 2016). ELISA is based on specific antibody-antigen binding (Singh et al., 2013). The detection is rapid after enrichment culturing; e.g., the commercially available Solus Scientific Solutions Ltd. can detect *Salmonella* in 36 h (W Stimson - US Patent App. 12/737, 2011). From food industry prospective, the long testing time increases the product cost due to the additional cost of storage and labour needed to transport the products. In addition, the time of testing may cut into a product's short shelf life. Releasing the products before the results are known will jeopardize the company's reputation and will cause significant economic losses if an outbreak or disease has spread.

Over the last twenty years, many pathogen diagnosis methods have been developed to detect *Salmonella* and other pathogen types to achieve the main goal of rapid detection. Those methods include electrochemical (Li et al., 2015; Dastider et al., 2013; Dweik et al., 2012; Ghosh Dastider et al., 2015, 2012; Jasim et al., 2017), optical (Yoo and Lee, 2016), Surface Plasmon Resonance (SPR) (Melaine et al., 2017; Nguyen et al., 2015), Mass-based biosensors (Singh et al., 2013), such as a quartz crystal microbalance (Ozalp et al., 2015), and electrical detection techniques (Zeeshan et al., 2018), and many other techniques (Tokel et al., 2015). As an example, an impedance biosensor was used to differentiate and detect *Salmonella* and *E-Coli based on* the difference in the adhesion properties of the pathogens to specific magnetic beads. By applying both magnetic and electric field, the pathogenic cells with negative surface charge was pushed to the positive side while the speed of bacteria was reduced resulting in impedance increase and limit of detection limit (LOD) of 100 cells/ml (Zeeshan et al., 2018). Interdigitated microelectrodes (IDMs) were also utilized for the detection of *E-Coli* and *Salmonella* in food products. For example, for separation, magnetic beads (MBs) were used and a screen-printed IDM was used for pathogen detection. The target molecules bound with antibodies that were immobilized on the IDM causing the capacitance to change. The LOD was 100 cells/ml (Xu et al., 2016). Graphene was also used with interdigitated electrodes to provide high carrier mobility and biocompatibility with antibodies and bacteria for the detection of *E-Coli O157:H7* with detection limits of 10–100 cells/ml (Pandey et al., 2017). A fiber optic immunosensor based on polystyrene waveguide and labeled bio-recognition molecules was used for pathogen detection with a LOD of 1000 cells/ml in 12 h (Abdelhaseib et al., 2016). Other rapid methods involve the use of SPR for the detection of *E-Coli* and *Salmonella* in hamburger and cucumber samples. A secondary antibody and gold nanoparticles were used for the sensitive and specific detection of low levels of *E-Coli* and *Salmonella*. The device was able to detect 17 CFU/ml for *E-Coli* and 7000 CFU/ml for *Salmonella* with total testing time of 80 min (Vaisocherová-Lísalová et al., 2016). Photoelectrochemical (PEC) sensing system was also implemented for the detection of prostate-specific antigen (PSA) using photoactive material. Reduced graphene oxide BiFeO3 (rGO-BiFeO3) was used as photoelectrode material. The detection limit of the device was 0.31 pg/ml with high selectivity and accuracy (Zhou et al., 2018). Another research group used a core–shell $NaYF_4$:Yb,Tm@TiO_2 upconversion microrods for the detection of carcinoembryonic antigen (CEA). Aptamer is first coupled with magnetic beads then functionalized with the CEA antigens. The primer DNA conjugated with the second aptamer starts the RCA reaction, which results in the formation of a long G-rich oligonucleotide strand. The resulted element releases numerous individual guanine (G) bases which increases the photocurrent under the near infrared light excitation. The detection limit was around 3.6 pg/ml (Qiu et al., 2018). Although these methods have shown good performance, they were not commercialized. This might be due to the complexity of some of the techniques, did not meet AOAC standard, and/ or other factors need to be considered when developing a rapid pathogen system. Those include cost, food matrices need to be tested, detection concentration requirements and the related sample volume. Rather than creating a zero-tolerance standard for raw poultry the USDA maintains a minimum number of samples that must be collected from broiler carcasses. Therefore, there is no required minimum number of bacterial cells/ml for raw poultry products to be considered unsafe to distribute. The number varies from one type of poultry product to another, and from one pathogen type to another. On the other hand, USDA/FDA set a zero-tolerance policy for ready to eat (RTE) products where the testing method must be able to detect 1 cell/325 g (Federal Register:: New Performance Standards for Salmonella).

This paper presents the design, fabrication and testing a MEMS impedance biosensor for rapid and simultaneous detection of multiple *Salmonella* serotypes with high specificity and sensitivity at a concentration as low as 7 cells/ml in poultry products in less than 40 min. The device uses three microchannels for the simultaneous detection of three *Salmonella* serotypes; each channel has a focusing region, and a sensing region. The sensing region is based on antibody-antigens binding process. As target *Salmonella* binds to the anti-*Salmonella* antibody, it results in impedance change. This change in impedance indicates the presence of bacteria cells.

2. Materials and methods

2.1. System design

The biosensor design is based on multiple microfluidic channels, each one consists of the following innovative features. (Fig. 1a): (1) A focusing region (length, and thickness are 3 mm, 25 μm, respectively) is designed to significantly improve the focusing capability of the device by getting rid of over 86% volume of the testing media. This results in a concentrated sample, significantly improves the pathogen detection sensitivity. This region consists of a ramp down vertical electrode pair along with tilted (with 45°) thin film finger pairs (200 pairs) with a ramp down channel. The finger's width and spacing between them, and spacing between the inner edges of the finger pairs, were 10 μm, and 10 μm, 10 μm, respectively. It generates p-DEP and hydrodynamic forces to focus and concentrate the *Salmonella* cells into the centre of the microchannel, and direct them toward the sensing microchannel. The width of each finger and the spacing between two adjacent fingers is 10 μm, and 10 μm, respectively. The width of each microchannel starts at 300 μm and then starts to decrease gradually to 100 μm at the focusing channel. The channel then splits into three narrower microchannels with equal width of 33 μm. The centre microchannel is where the detection electrodes are located and the two side microchannels are used to get rid of the bulk media. (2) A sensing region for bacterial cells detection which consists of three set of interdigitated electrode (IDE) arrays, each array has number of fingers equals to 10 pairs to facilitate the detection of very low concentration of bacteria. The total height of the channel is 25 μm. Initially, three types of *Salmonella* antibodies (type B, D and E) were mixed separately with the cross-linker sulfo-succinimidyl 6-(3′-(2-pyridyldithio) propionamido) hexanoate (Sulfo-LC-SPDP) to increase the adhesion efficiency between antibodies and the substrate. The electrode surfaces were then functionalized with the three mixtures, one for each microchannel and without causing any cross contamination by using three different inlets. Poultry samples (raw chicken and turkey ready to eat (RTE)) spiked with *Salmonella* type B were injected into the biosensor via the sample main inlet towards the focusing region. The injected sample was focused using an applied AC signal in each microchannel to the focusing electrodes to

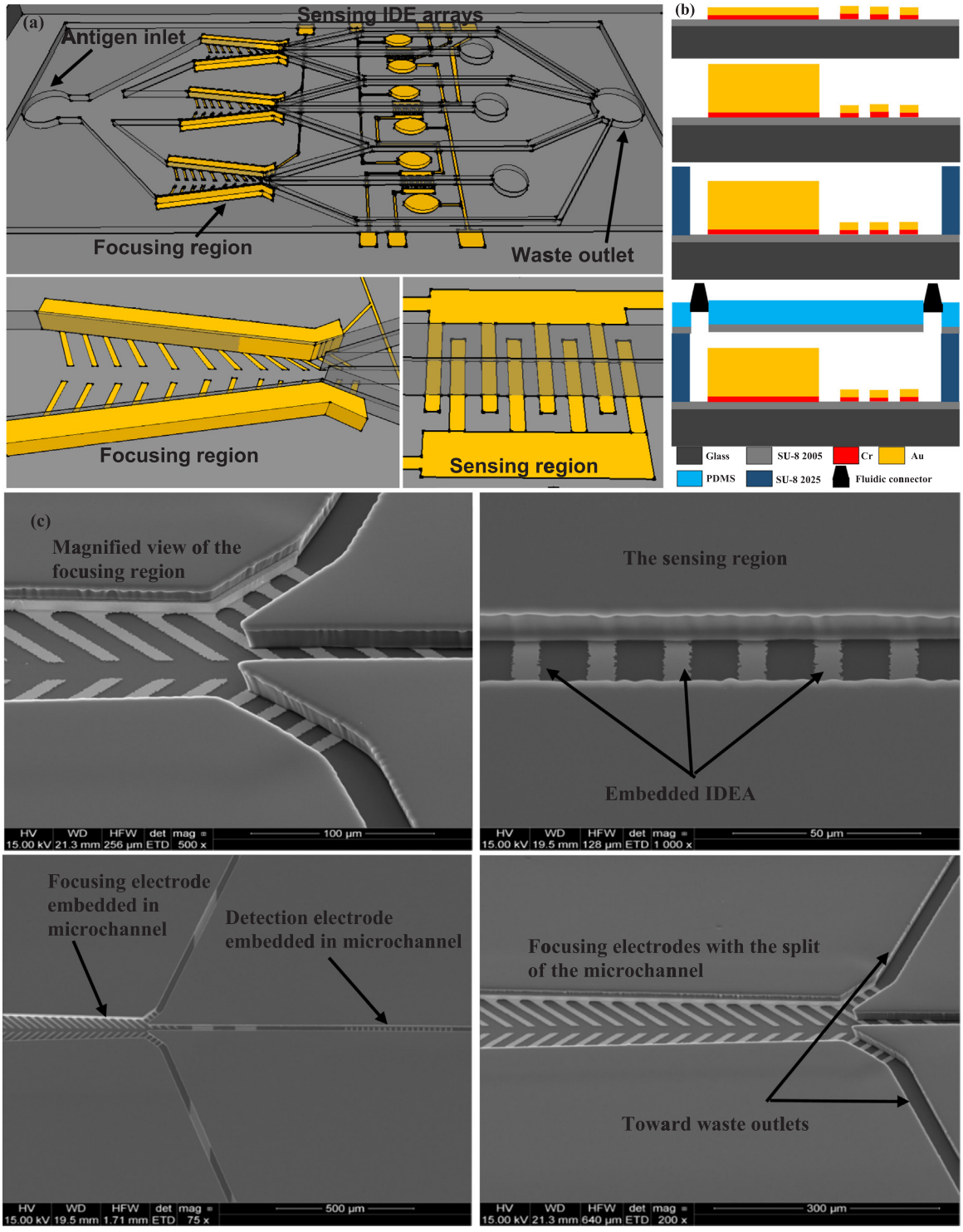

Fig. 1. (a) Schematic images of the impedance based biosensor, magnified view showing the focusing electrode, and magnified view of the detection electrodes. (b). Cross sectional view showing the fabricated layers of the biosensor which includes patterned thin film electrodes, electroplated vertical walls, SU8 2025 microchannel, and PDMS cover and fluidic connectors. (c) SEM micrographs of the fabricated device showing magnified view of the fabricated focusing region, magnified view of the fabricated detection region, focusing and detection region, and the focusing region showing the split of the microchannel.

generate non-uniform E-field. This applied p-DEP along with the fluidic drag effect push *Salmonella* cells and focus them toward the centre of the microchannel which is directed to the sensing region. Cells were left on top of the IDE array surfaces for 30 min to facilitate the binding between *Salmonella* antibodies and antigens which results in change in impedance.

2.2. Device fabrication

The fabrication of the device was performed on a glass slide with dimension 2 × 1.5 in. using several steps of surface micromachining technology as shown in Fig. 1b. The process starts with (1) cleaning the glass slides by putting the substrates in a piranha bath hydrogen peroxide (H2O2) and sulfuric acid (H2SO4) at a ratio of 1:3 respectively

for 5 min. The goal of piranha cleaning is to remove all the organic particles and residues. The samples were then washed thoroughly with deionized (DI) water and blown dry with a nitrogen gas. (2) SU-8 2005 (Microchem) photoresist layer was spin coated with a thickness of 4 μm onto the glass slides, prebaked, flood exposed, post baked and finally hard baked at 150 °C for 30 min. This layer will cover the whole slide to be used to enhance the adhesion between the subsequent SU-8 2025 channel and glass substrate to avoid channel peeling off from the substrate. (3) Two thin layers of chromium (Cr) and gold (Au) were deposited on top of the SU8 layer with thicknesses of 50 nm and 150 nm, respectively, using DC sputtering at 200 W for Cr and 90 W for Au. The Au thin film was patterned to form the IDE array, the electrode traces, bonding pads, focusing fingers and electroplating seed layer. Wet etching was performed to pattern the Au layer using potassium iodide (KI) and iodine (I2) mixture. (4) Creating a mold for electroplating gold side walls for the focusing electrodes. This was done by spin coating and patterning AZ 4620 photoresist with a 12 μm thickness. Followed by immersing the device into Technic gold 25 ES gold electroplating solution to plate the Au on the focusing electrodes locations. The electroplating solution was placed on top of a hotplate and heated at 55 °C, stirred at a rate of 75 rpm and 60 μA current was applied for 6 h. The resulted thickness of the electroplated structure was 12 μm. The AZ photoresist mold was no longer needed thus, it was removed using acetone, isopropanol 2 (IPA), and DI water. Followed by removing the Cr layer by using Cr etchant for 30 s followed by DI wash bath as shown in. (5) The patterning of the SU8 2025 to create the microchannel. The process starts with spin coating SU8 2025, followed by prebake, UV exposure, post bake, development and finally hard bake. The last step in fabrication is the polydimethylsiloxane (PDMS) bonding to seal the microchannel. (6) Two (PDMS) slabs were prepared and cured to serve as top cover for the microchannel with fluidic connectors for the inlets and outlets. Two PDMS covers were used. The first cover was cut and punched manually and then cured and exposed to oxygen plasma to make the surface hydrophilic so that SU8 2005 layer can be treated on the surface. Then SU8 2005 was spin coated on the PDMS and baked at 95 °C in oven. After that the PDMS cover was manually aligned and bonded to the device and baked at 48 °C on a hotplate. A weight was placed on the device to improve the bonding strength. This was followed by the second PDMS cover with fluidic connectors. The PDMS cover was exposed to oxygen plasma, aligned and bonded to the device manually. (7) To improve the device reliability and to eliminate any possible fluid leakage, the fluidic connectors were further sealed using epoxy glue. Finally, the device was wire bonded to an external PCB board which was connected to an impedance analyzer, Agilent 4294A. This process facilitated the impedance measurement procedure and ensure reliable and accurate results. Scanning electron micrographs of the fabricated devices are shown in Fig. 1c, and a package device is shown in Fig. 2a.

2.3. Modelling and simulation

Using COMSOL finite element tool, the electric field (E-Field) intensity and its gradient were simulated across the focusing electrodes using AC voltage (Vp-p = 6 V) at a specific frequency (6 MHz). The results demonstrated that E-field and its gradient are highest at the centerline of the microchannel, and decreases significantly while moving away towards the microchannel walls (Fig. 3a). Therefore, when pathogenic cells or microbeads are injected into the microchannel, the E-field gradient (at specific frequency and AC voltage) generates positive dielectrophretic forces (pDep) that pushes the cells toward the centerline of the microchannel, and direct them toward the detection zone microchannel which has a width, 33 μm, much smaller than the opening of the focusing microchannel, i.e., 300 μm. The bulk fluid will keep flowing toward the outer channel into the waste outlets. Initially, the tilted thin film finger pairs will generate larger p-DEP forces, dominating the focusing process because the vertical sidewalls

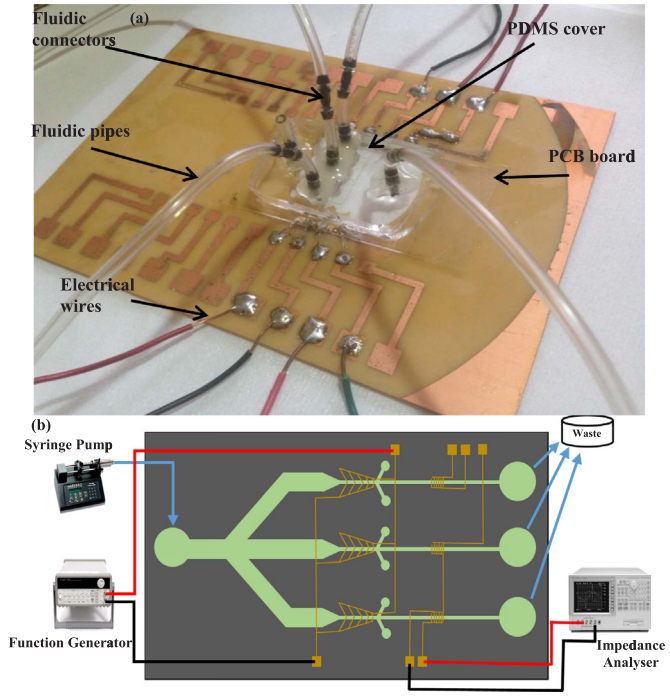

Fig. 2. (a) Completely fabricated bonded biosensor to a PCB board showing the fluidic connectors and tubes. (b) A schematic of the *Salmonella* testing setup. It consists of syringe pump, function generator, impedance analyzer, and the fabricated biosensor.

are far from each other, and thus focusing the cells in a narrow line in the centre (about 10 μm wide). As the channel ramps down, the generated p-DEP force from the vertical electrode pair becomes more dominants especially in the z-axis and contributing more to the focusing process. In addition, the ramp down feature of the channel will generate hydrodynamic forces that will also aid the focusing process (Fig. 3b). However, the hydrodynamic forces alone will not be able to focus the cell into the centerline unless the microchannel is very long. We have also simulated the fluid velocity distribution along the focusing region which shows the increase in fluid speed gradually as the width of the focusing channel decreases gradually. Although the velocity in the figure shows a parabolic behavior throughout the focusing channel, the velocity distribution at the end of the channel, where the main channel split into three smaller ones, is not parabolic. This was demonstrated by the red color in the three microchannels. Therefore, no focusing is happening.

2.4. Impedance measurement

The testing starts with flowing three types of *Salmonella* antibodies mixed with cross-linker separately, one type from each inlet. After the three mixtures of antibodies (types B, D and E) were immobilized on the detection electrodes, one type in each channel, the channel was washed with water to remove the unbounded antibodies. Then, the impedance of each IDE array was measured using the impedance analyzer over a range of frequencies from 100 Hz to 10 MHz. Then *Salmonella* type B were injected to the sample inlet. After the channel was filled, the flow was stopped for 30 min to allow the binding between the *Salmonella* antigens (type B) and *Salmonella* antibodies (type B). After cleaning the channel with water, the impedance was measured again in each channel over the same range of frequencies. The difference of impedance between the antibodies and the antigens readings indicates the presence or absence of bacterial cells. The total testing time is 40 min and can only do one testing for each device. The antibodies coating time is not included because the future product is supposed to be a

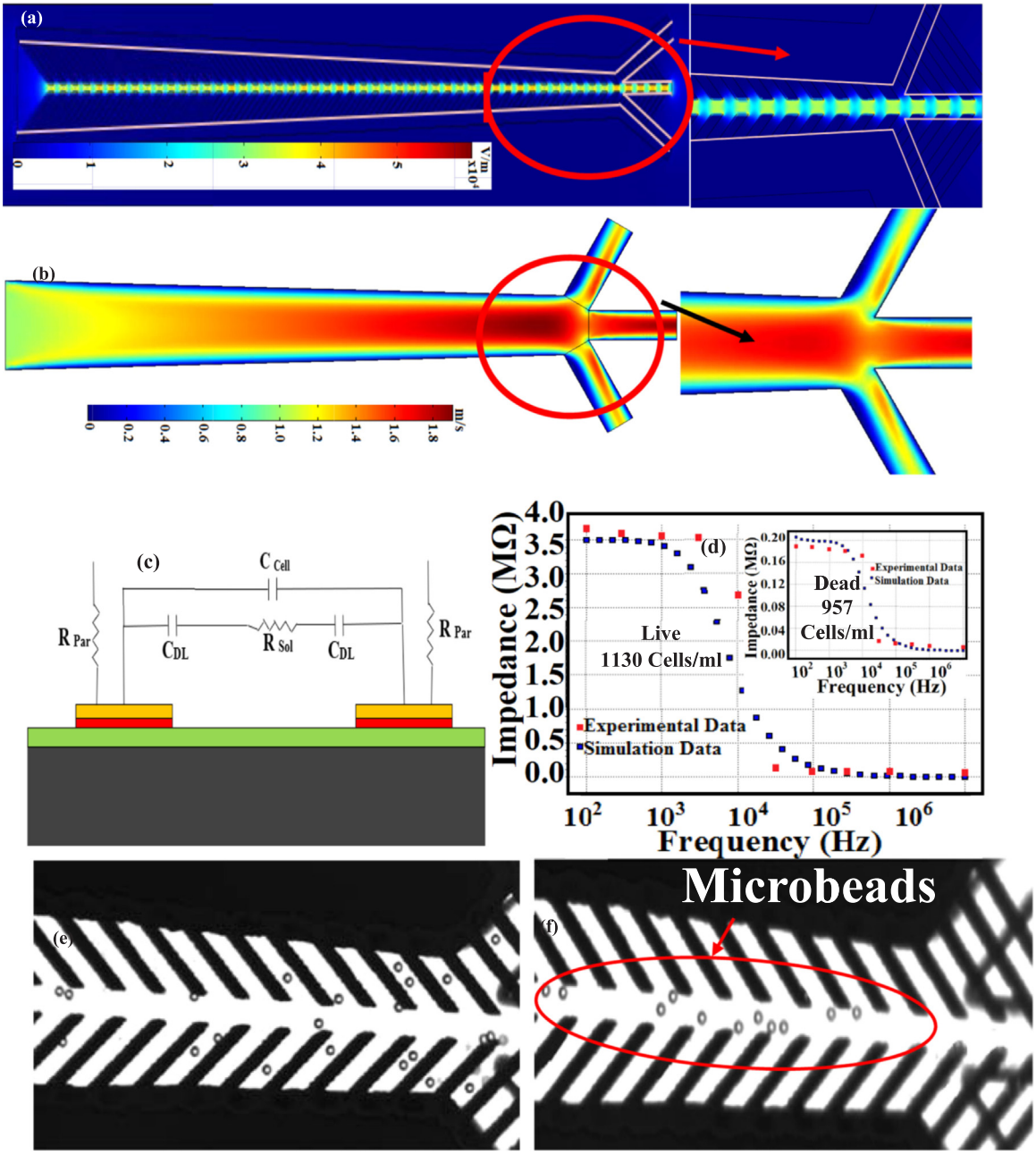

Fig. 3. (a) The simulation of the electrical field across the length of the focusing region. (b) The velocity modelling showing the fluid velocity along the focusing channel. (c) Equivalent circuit of the impedance based biosensor showing the circuit components. (d) The simulation of the equivalent circuit and the experimental results showing the impedance response over medium and high frequencies region for live and dead cell. (Bottom) Optical image of the focusing region (e) no focusing effect is applied and the microbeads are everywhere in the channel. (f) Focused microbeads in the centre of the microchannel under the influence of the p-DEP force.

disposable. Therefore, it will be pre-coated with antibodies before sale. Various samples of ready to eat (RTE) turkey and raw chicken were spiked with *Salmonella* type B with various concentrations and were tested.

3. Results and discussions

3.1. Theory

The device uses positive Dielectrophoresis (DEP) for focusing the antigens. DEP can be defined as the forced motion of small dielectric particles or cells under the effect of non-uniform AC electrical field in a suspending medium. The cell or particle is directed by the non-uniform electric field (E-field) force towards the region of minimum or maximum electrical field. The particle permittivity compared with that of the surrounding medium and the frequency of the applied electrical field define the direction of the driving force. In this project, the applied E-field magnitude and frequency were adjusted such that the cells were pushed toward the centre of the focusing electrode where the E-field is high (pDep), and continue flow toward the detection region. The bulk media that does not contain *Salmonella* exit from the outer two channels toward the waste outlets. This has resulted in a concentrated sample. The dielectric force (FDEP) on a homogeneous spherical particle can be expressed by the following equation:

$$F_{DEP} = 2\pi\varepsilon_m r^3 \nabla E^2 \mathrm{Re}[K(\omega)]$$

where r is the radius of the sphere and in our case the radius of the cell, ε_m is complex permittivity of medium, E is value of the E-field. $K(\omega)$ is called the Clausius-Mossotti (C-M) factor. To attract the cells to the sensing region, p-DEP is generated by adjusting the frequency of the applied E-field which changes the value of $K(\omega)$. The other force that pushes the cells to the centre of the focusing region is the hydrodynamic force due to the ramp down shape of the channel (Paredes et al., 2014).

3.2. Equivalent electrical circuit

To analyze the impedance response of the detection electrode, the equivalent circuit of the biosensor in the solution and in the presence of live and dead *Salmonella* cells was studied and represented by the circuit shown in Fig. 3c. The electrode pair, each with an area S and spacing D, were placed in parallel. Thus, when an AC voltage (v) was applied to the electrode pair, a current was flown, and the solution resistance R_{Sol} was:

$$R_{Sol}=\frac{v}{i}\rho_{Sol}\frac{D}{S} \quad (1)$$

The solution resistance, which is proportional to the solution resistivity ρ_{Sol} connected in series with two double layer capacitors of the interdigitated electrode array (C_{DL}). The testing sample solution resistance R_{Sol} between the interdigitated electrode pair is proportional to the concentration of the pathogen in the tested sample. Both C_{DL} and R_{Sol} are connected in parallel with the dielectric capacitance (C_{Cell}) of the interdigitated electrodes, which depends on the solution dielectric constant and the geometry of the electrodes. The parasitic resistors (R_{Par}) are generated from the connections and wires of the measuring circuit which is small and can be neglected. Current will flow through the R_{Sol} while another current called a displacement current flow through the capacitor C_{Cell}. The total impedance of the circuit is equal to the summation of the R_{Sol} and the two capacitors C_{DL} impedance. The total impedance is expressed by:

$$Z\approx\frac{2+j\omega.C_{DL}.R_{Sol}}{J.\omega.C_{DL}} \quad (2)$$

$$C_{DL}\approx\frac{\varepsilon_r\varepsilon_o S}{D} \quad (3)$$

where ε_r is the solution relative permittivity. At low frequency, the impedance is dependent on the double layer capacitance C_{DL} until the impedance of this capacitor becomes lower than the R_{Sol}. At medium frequency (100 Hz to 10 kHz), the CDL has no effect on the total impedance and the impedance is mainly dependent on the resistance of the solution (Ibrahim et al., 2013; Zang et al., 2016).

The equivalent circuit was simulated using EIS spectrum analyzer to show the response of the circuit in case of testing live cells and dead cells. The value of the C_{DL} is calculated to be 20 nF, and the value of the R_{Sol} is basically the value of the tested solution which is calculated to be 200 kΩ for the dead cells with concentration of 957 cells/ml, and 3.5 M Ω for the live cells with concentration of (1130 cells/ml). R_{Sol} of the dead cells sample is small because of the significantly low number of *Salmonella* cells bind to the electrodes. In the contrary, R_{Sol} is big in the case of live *Salmonella* cells because of the high number of cells bind to the detection electrodes. Fig. 3d shows the simulation result of the equivalent circuit where clearly identify the two distinct regions of the impedance response. The region of medium frequency where the R_{Sol} is dominant and the impedance is frequency independent. At frequency, above 10 kHz, current will only flow through C_{Cell} which defines the impedance value. The reason that the dead cells show low impedance is that since the antigens on the dead cell surface are damaged or compromised, the specific binding between the immobilized antibodies and the antigens cannot be formed or weakened. Unbound dead cells are then washed away during the cleaning process thus will not change the resistance of the solution during the dead cells testing compared with the base reading of the solution resistance of the electrodes immobilized with antibodies.

3.3. Testing setup

The experimental setup that was used to test the device for the presence/absence of *Salmonella* cells is shown in Fig. 2b. Three syringe pumps (a Harvard Apparatus PHD 2000) are used to inject three types of antibodies, and 1 syringe pump is used to inject the *Salmonella* antigens samples. An inverted microscope was used with an installed CCD camera to capture optical images of the device during the testing. To generate p-DEP forces, a function generator was used to apply an AC voltage across the focusing electrodes. Finally, an impedance analyzer (Agilent 4294A) was used to perform precise measurements of the impedance across the detection electrodes. The impedance values were measured for a range of frequencies between 100 Hz and 10 MHz.

3.4. Focusing effect

Polystyrene microbeads with a diameter of 4 μm were used to test the focusing capability of the device. One drop of the microbeads mixed with 1 ml of DI water was injected from the device inlet. An AC signal was applied across the focusing electrodes. The amplitude and the frequency of the applied AC signal were experimentally adjusted to optimize the generated pDep forces such that the microbeads/ bacterial cells are pushed toward the centre of the microchannel. The testing results using microbeads with diameter of 4 μm before and after applying the pDep effects is shown in Fig. 3(e, f). The results demonstrate that the microbeads are flowing randomly everywhere in the microchannel before applying the pDep effect, but when the pDep effects were applied the microbeads moved to the centreline. This demonstrates that the pDep is the dominant force that caused the focusing of beads. In addition, the device was tested with and without the use of the focusing electrodes to demonstrate its impact on the detection results. From the simulation results and the conducted experiments, it was found that 6 V peak-to-peak at 6 MHz AC signal gave the best focusing results.

3.5. Sample preparation

Rabbit anti-*Salmonella* antibodies poly B, D, and E were purchased from Becton, Dickinson and Company, USA. The antibodies were 1:100 diluted with the solution of the negative control spiking. RTE turkey breast sterile deionized water. The crosslinker, sulfosuccinimidyl 6-[3-(2-pyridyldithio) propionamido] hexanoate (sulfo-LC-SPDP), was used for antibody immobilization. The mixture was then loaded into the biosensor. The flow was stopped for 1 h to allow the antibodies to be immobilized on the three electrodes arrays.

Ready-to-eat (RTE) turkey breast was purchased from grocery stores and stored at 4 °C until use. An avirulent *Salmonella* enterica Typhimurium strain (ΔsipB, cat +) was used to spike RTE turkey breast. RTE turkey breast was weighted and each 25-g sample was placed into a sterile bag. One millilitre of the above bacterial suspensions was directly added to the RTE samples in the bags to make the spiked samples containing 10°, 10^{1}, and 10^{2} CFU *Salmonella* cells per 25 g respectively. A negative control was prepared by adding 1 ml of sterile buffered peptone water (BPW) into a 25-g RTE sample. After waiting for 5 min, 225 ml of sterile buffered peptone water (BPW) was added into each bag and the bags were incubated at 37 °C for enrichment. After 4 h, a 50-ml solution will be withdrawn from each of the bags and passed through a 20-mm filter to remove food debris which might block the device channel. Filtered solution were mixed with 100% glycerol at the ratio of 3:1 and then frozen at – 80 °C for future use. 1 ml of the solution can be drawn and loaded to the device. *Salmonella* concentrations of the samples were examined and counted by plating the samples for each experiment.

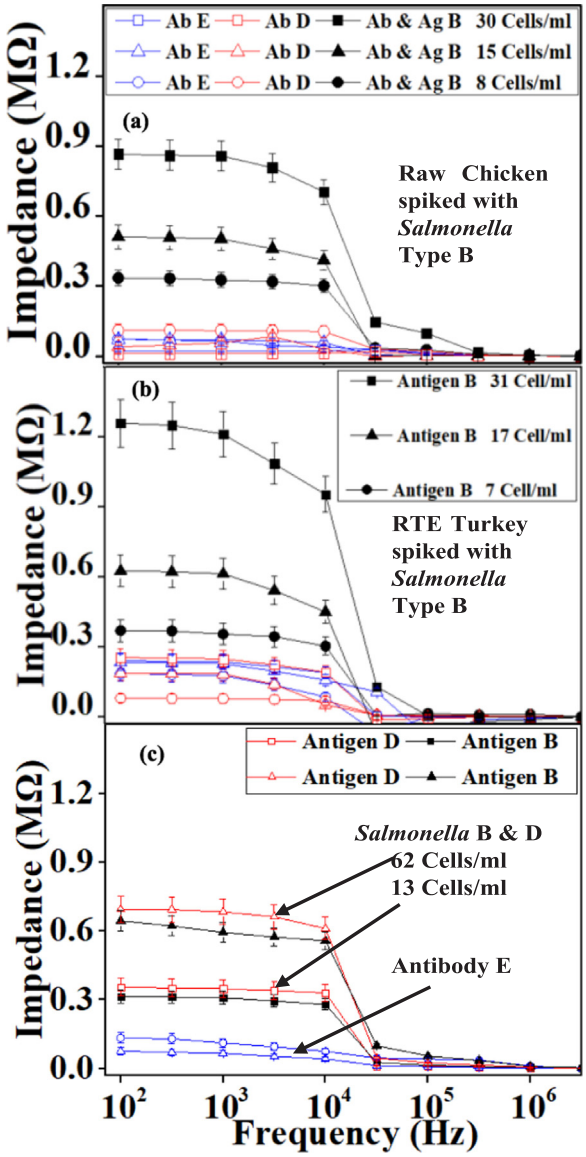

Fig. 4. Testing results of Salmonella with two different food matrices. Three types of antibodies (B, D, and E) were mixed with cross-linker and flown into the device separately without any cross contamination. The testing was performed with the focusing effect. (a) Raw chicken with concentrations of 7, 19, 42 cells/ml. (b) RTE turkey with concentrations of 8, 17 and 45 cells/ml. The comparison is different between Raw chicken and RTE Turkey matrices(c) Testing device ability to detect *Salmonella* type B and D serogroups simultaneously by flowing two equal quantities mixture of the two different *Salmonella* serogroups for 62 cells/ml and 13 cells/ml concentrations.

3.6. Testing results

The testing results are shown in Fig. 4(a, b) for several concentrations for the two matrices. The figures were plotted with error bars. Each error bar represents testing of 1 *Salmonella* concentration three times using three different devices. Each device was used only once (disposable devices). The lowest measured concentration for RTE Turkey and raw chicken were 7 and 8 cells/ml respectively. For each tested sample, the cell count was defined by the gold standard method which is cell culture. The selection of the cell counts was not random. For example, the prepared solution was targeting *Salmonella* with a concentration of 10 cells/ml. From this solution, one sample was used for device testing, while the second sample was used for bacterial culture (24 h) in order to provide the actual cell counts. This actual cell count was not precisely 10 cells/ml but it was close, for example, 8 cells/ml, or 12 cells/ml. For accuracy, the exact number of cells obtained from the culture experiment were reported. The biosensor doesn't perform pathogen cell count; however, it can tell the presence/absence of bacterial cell. The strength of the signal may indicate a concentration range. At the time of testing, part of the tested sample was cultured to count the number of pathogen cells in the testing sample for confirmation. The results demonstrated the device ability to detect low concentration selectively. The other two channels that were coated with *Salmonella* antibody type E and D have weak signal. This indicates high specificity of the device. The device was also tested using RTE turkey samples that were spiked with two types of *Salmonella* serogroups while the detection electrodes were coated with anti-*Salmonella* antibodies type B, D, and E. This was performed by flowing a mixture of two equal quantity types of *Salmonella* serogroups (type B and D) into the device. The results shown in Fig. 4c, shows strong signal for two channels that were coated with matching antibodies while the third channel that was coated with *Salmonella* type E showed weak signal. This confirmed the device capability to do detection of multiple pathogens.

The device was tested with and without the use of the focusing electrodes to demonstrate its impact on the detection results. Fig. 5(a, b) shows a comparison between the focusing and the non-focusing effect for *Salmonella* type B. The results show that the use of the focusing region has improved the signal by a 4–6.25 times. The device selectivity was tested. This was accomplished by coating the detection electrodes with three types of *Salmonella* antibodies (B, D and E) in the three channels while the pathogenic sample was raw chicken spiked with *E-Coli* O157:H7 and injected via the sample inlet. From the results in Fig. 5(c, d), the measured impedance values are similar to the baseline impedance. This clearly indicate the device ability to selectively detect *Salmonella* selectively.

The device ability to differentiate between live and dead *Salmonella* was also tested. The *Salmonella* type B were killed by brief exposure of cells to heat. The tests were performed by flowing dead *Salmonella* into the device and determine the impedance chance. For the tested dead cells, the generated signal was low and comparable to the impedance value measured without the presence of *Salmonella* (See Fig. 6(a, b)). The lowest concentration of *Salmonella* (8 cells/ml) in raw chicken samples, dead cells and non-specific binding *E-Coli* were plotted in the same figure in order to show clearly the difference in impedance values (see Fig. 6b inset). The figure demonstrates that the lowest concentration of *Salmonella* can be differentiated successfully from the dead cells and non-specific binding *E-Coli*. SEM micrographs of both live and dead cells can be seen in (Fig. 6c and d live cells and e, single dead cell). Since the antigens on the dead cell surface are damaged or compromised, the specific binding between the immobilized antibodies and the antigens cannot be formed or weakened. Unbound dead cells are then washed away during the cleaning process, and thus resulting in the change in impedance relatively small.

The device has multiple advantages which includes limit of detection, required detection time, and ability to simultaneously detect multiple pathogens or *Salmonella* serogroups. With this level of sensitivity, the device can be used for process control in slaughter processing plants to detect *Salmonella* in raw poultry products in < 1 h without the need for a sample enrichment step due to the absence of zero tolerance requirement. However, for RTE poultry products, the USDA/FDA set a zero-tolerance requirement, i.e., 1 cell/325 g of product. Therefore, use of our device for RTE poultry products will require a short enrichment step. The length of the enrichment culture will be much shorter than with other technologies, such as ELISA and PCR, due to the high sensitivity of our device. In experiment, approximately 32.5 *Salmonella* cells were inoculated on 325 g RTE Turkey and enriched in 975 ml BPW at 1:4 dilution and at 37 °C. After 2 h, the *Salmonella* concentration reached 7 Cells/ml. In a second experiment, 5 *Salmonella* cells were inoculated on 325 g RTE Turkey sample. In this case, it took 6 h to reach

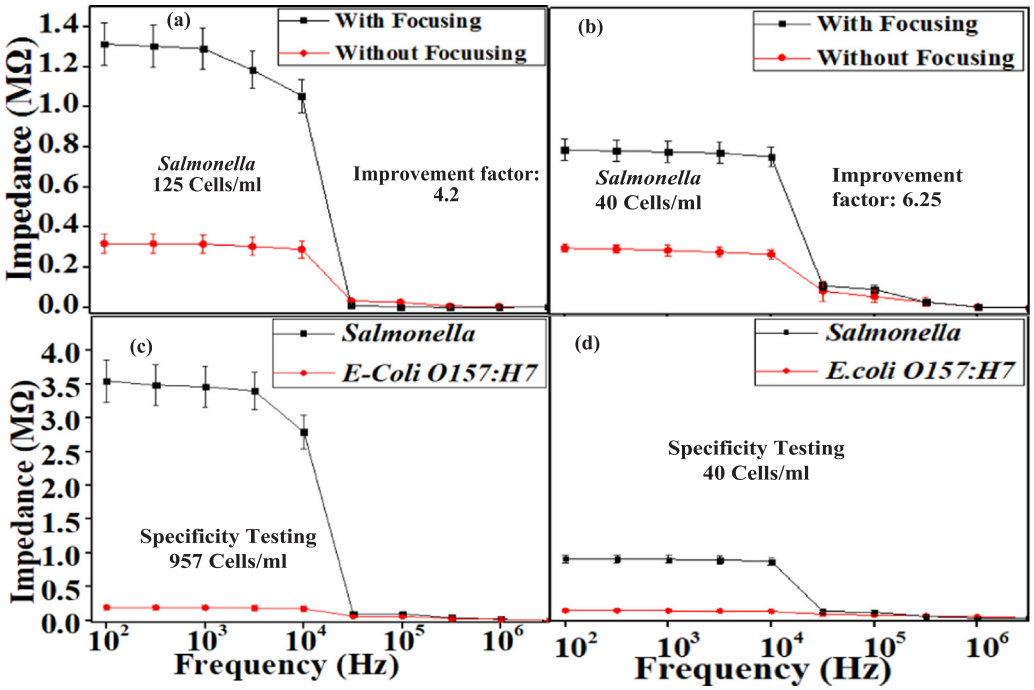

Fig. 5. (Top) Detection of *Salmonella* type B with and without focusing effect for (a) 125 cells/ml, (b) 40 cells/ml. The testing results demonstrate that the addition of focusing region has improved the signal strength by a factor ranged between 4 and 6.25. (Bottom) Selectivity testing to specific *Salmonella* type B for concentration of (c) 957 cells/ml, (d) 40 cells/ml. The results show the device ability to only detect *Salmonella* type B and no other types of pathogens such as *E-Coli*. This was performed by flowing *E-Coli* into the detection region immobilized with *Salmonella* antibody.

a concentration of 12 cells/ml. The low limit of detection (8 Cells/ml) indicates that our device will be able to approach the 1 cell/325 g requirement within a production plant shift.

4. Conclusions

In this paper, we presented an impedance-based MEMS biosensor for simultaneous detection of multiple *Salmonella typhimurium* serogroups in poultry products (raw chicken and ready to eat (RTE)

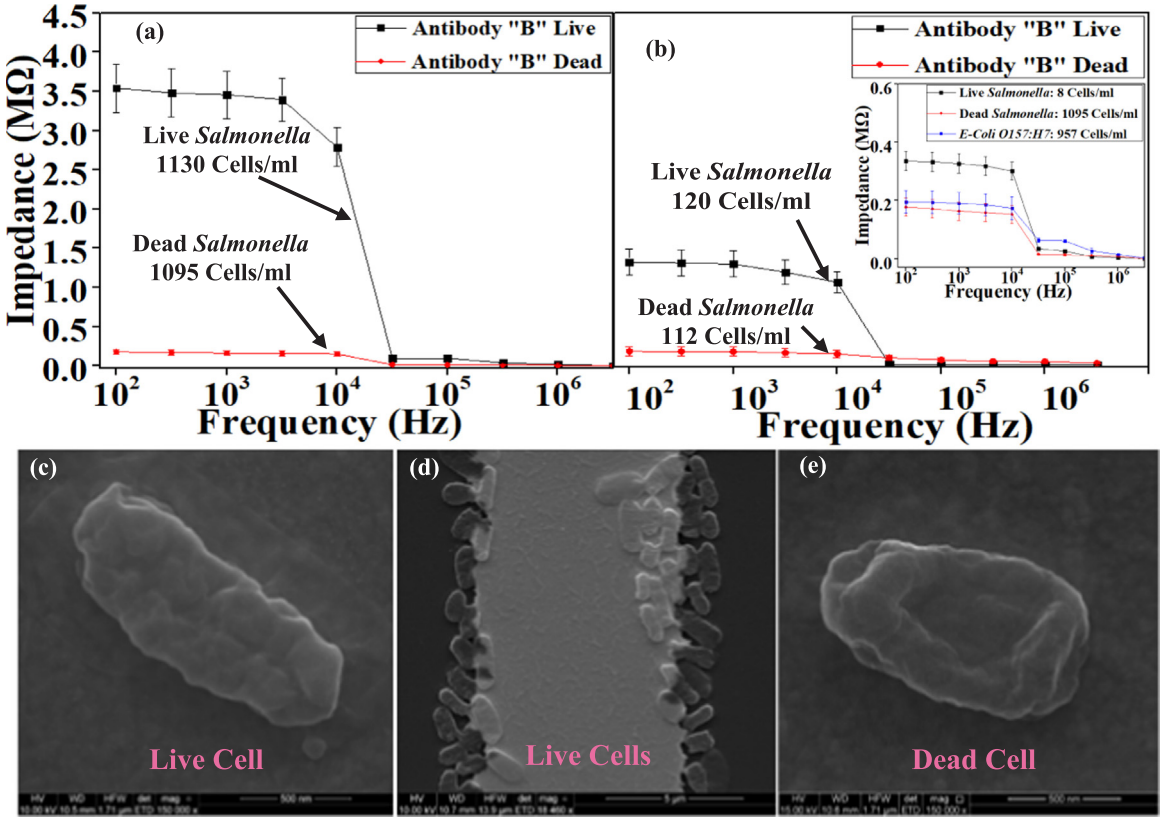

Fig. 6. (Top) Comparison between live and dead *Salmonella* cells for high concentration (a) 1100 Cells/ml and (b) 120 Cells/ml. (b) Inset A comparison between low concentration of live *Salmonella* cells (8 cells/ml), *E-Coli* (957 cells/ml) and dead *Salmonella* cells (1095 cells/ml) using raw chicken samples. The results demonstrate the device capability to differentiate between live and dead cells. (Bottom) SEM micrographs of live and dead cells placed on the interdigitated electrode array (c, d) live intact *Salmonella* cells, (e) Single dead *Salmonella* cell showing a hole in the centre of the cell.

Turkey). The impedance of each electrode in the three detection regions was recorded after coating with a mixture of anti-*Salmonella*-antibodies (B, D, or) and cross-linker, independently without causing cross-contamination, and after injecting the bacterial sample. The antibody impedance was then subtracted from the total impedance to determine the *Salmonella* cells impedance alone. By changing the antibody coating, the device can be used for detection of other pathogens. The testing results demonstrates that the use of pDep effects resulted in a concentrated *Salmonella* sample in the detection channels, which increased the device sensitivity by a factor between 4 and 6.25, and thus it enabled the device to achieve a detection limit as low as 7 cells/ml with a detection time of 40 min. The device was tested successfully in the presence of two *Salmonella* serogroups (B, and D) too. In addition, the device was able to detect and differentiate *Salmonella B* at low concentration selectively in the presence *E. coli O157:H7*, and dead *Salmonella* cells at low and high concentrations. The device can be used for process control in slaughter processing plants to detect *Salmonella* in raw poultry products in less than 1 h without the need for a sample enrichment step while for RTE poultry products, a short sample enrichment step is required.

Acknowledgements

This project is supported in part by Coulter Foundation/ MU partnership.

Conflicts of interest

There are no conflicts to declare.

References

World Health Organization, The World Health Report 2004, World Health Organization, Genève, 2004. Google Search [WWW Document], n.d. URL 〈https://www.google.com/search?Q=1+World+Health+Organization%2C+The+World+Health+Report+2004%2C+World+Health+Organization%2C+Genève%2C+2004.&rlz=1C1GCEB_enUS748US748&oq=1+World+Health+Organization%2C+The+World+Health+Report+2004%2C+World+Health+Organi〉. (Accessed 5 January 2018).

Abdelhaseib, M.U., Singh, A.K., Bailey, M., Singh, M., El-Khateib, T., Bhunia, A.K., 2016. Fiber optic and light scattering sensors: complimentary approaches to rapid detection of Salmonella enterica in food samples. Food Control 61, 135–145. https://doi.org/10.1016/j.foodcont.2015.09.031.

Brenner, F.W., Villar, R.G., Angulo, F.J., Tauxe, R., Swaminathan, B., 2000. Salmonella nomenclature. J. Clin. Microbiol. 38, 2465–2467.

Burden of Foodborne Illnesses in the United States, Estimates of Foodborne Illness, CDC [WWW Document], n.d. URL 〈https://www.cdc.gov/foodborneburden/burden/index.html〉. (Accessed 25 September 2018).

Dastider, S.G., Barizuddin, S., Dweik, M., Almasri, M., 2013. A micromachined impedance biosensor for accurate and rapid detection of E. coli O157:H7. RSC Adv. 3, 26297. https://doi.org/10.1039/c3ra44724c.

Dweik, M., Stringer, R.C., Dastider, S.G., Wu, Y., Almasri, M., Barizuddin, S., 2012. Specific and targeted detection of viable Escherichia coli O157:H7 using a sensitive and reusable impedance biosensor with dose and time response studies. Talanta 94, 84–89. https://doi.org/10.1016/J.TALANTA.2012.02.056.

Federal Register:: New Performance Standards for Salmonella, and Campylobacter in Not-Ready-to-Eat Comminuted Chicken and Turkey Products and Raw Chicken Parts and Changes to Related Agency Verification Procedures: Response to Comments and Announcement of Implementation Schedule [WWW Document], n.d. URL 〈https://www.federalregister.gov/documents/2016/02/11/2016-02586/new-performance-standards-for-salmonella-and-campylobacter-in-not-ready-to-eat-comminuted-chicken〉. (Accessed 22 September 2018).

Foodborne Illness and Disease [WWW Document], n.d. URL 〈https://www.fsis.usda.gov/wps/portal/fsis/topics/food-safety-education/get-answers/food-safety-fact-sheets/foodborne-illness-and-disease〉. (Accessed 5 January 2018).

Ghosh Dastider, S., Barizuddin, S., Dweik, M., Almasri, M.F., 2012. Impedance biosensor based on interdigitated electrode array for detection of Escherichia coli O157:H7 in food products. Int. Soc. Opt. Photonics. https://doi.org/10.1117/12.920821. (p. 83690Q–83690Q–7).

Ghosh Dastider, S., Barizuddin, S., Yuksek, N.S., Dweik, M., Almasri, M.F., 2015. Efficient and rapid detection of *Salmonella* using microfluidic impedance based sensing. J. Sens. 2015, 1–8. https://doi.org/10.1155/2015/293461.

Hyeon, J.-Y., Deng, X., 2017. Rapid detection of Salmonella in raw chicken breast using real-time PCR combined with immunomagnetic separation and whole genome amplification. Food Microbiol. 63, 111–116. https://doi.org/10.1016/J.FM.2016.11.007.

Ibrahim, M., Claudel, J., Kourtiche, D., Nadi, M., 2013. Geometric parameters optimization of planar interdigitated electrodes for bioimpedance spectroscopy. J. Electr. Bioimpedance 4, 13–22. https://doi.org/10.5617/jeb.304.

Jasim, I., Abdullha, A., Shen, Z., Zhang, S., Alalem, M., Dewik, M., Almasri, M., 2017. An impedance biosensor for simultaneous detection of low concentration of Salmonella serogroups in poultry samples. In: 2017 Proceedings of the 19th International Conference on Solid-State Sensors, Actuators and Microsystems (TRANSDUCERS). IEEE, pp. 726–729. 〈https://doi.org/10.1109/TRANSDUCERS.2017.7994151〉.

Li, Z., Fu, Y., Fang, W., Li, Y., Li, Z., Fu, Y., Fang, W., Li, Y., 2015. Electrochemical impedance immunosensor based on self-assembled monolayers for rapid detection of Escherichia coli O157:H7 with signal amplification using lectin. Sensors 15, 19212–19224. https://doi.org/10.3390/s150819212.

McGhie, E.J., Brawn, L.C., Hume, P.J., Humphreys, D., Koronakis, V., 2009. Salmonella takes control: effector-driven manipulation of the host. Curr. Opin. Microbiol. 12, 117–124. https://doi.org/10.1016/J.MIB.2008.12.001.

Melaine, F., Saad, M., Faucher, S., Tabrizian, M., 2017. Selective and high dynamic range assay format for multiplex detection of pathogenic *Pseudomonas aeruginosa*, *Salmonella typhimurium*, and *Legionella pneumophila* RNAs using surface plasmon resonance imaging. Anal. Chem. 89, 7802–7807. https://doi.org/10.1021/acs.analchem.7b01942.

Nguyen, H., Park, J., Kang, S., Kim, M., 2015. Surface plasmon resonance: a versatile technique for biosensor applications. Sensors 15, 10481–10510. https://doi.org/10.3390/s150510481.

Ozalp, V.C., Bayramoglu, G., Erdem, Z., Arica, M.Y., 2015. Pathogen detection in complex samples by quartz crystal microbalance sensor coupled to aptamer functionalized core–shell type magnetic separation. Anal. Chim. Acta 853, 533–540. https://doi.org/10.1016/J.ACA.2014.10.010.

Pandey, A., Gurbuz, Y., Ozguz, V., Niazi, J.H., Qureshi, A., 2017. Graphene-interfaced electrical biosensor for label-free and sensitive detection of foodborne pathogenic E. coli O157:H7. Biosens. Bioelectron. 91, 225–231. https://doi.org/10.1016/J.BIOS.2016.12.041.

Paredes, J., Becerro, S., Arana, S., 2014. Label-free interdigitated microelectrode based biosensors for bacterial biofilm growth monitoring using Petri dishes. J. Microbiol. Methods 100, 77–83. https://doi.org/10.1016/J.MIMET.2014.02.022.

Qiu, Z., Shu, J., Tang, D., 2018. Near-infrared-to-ultraviolet light-mediated photoelectrochemical aptasensing platform for cancer biomarker based on core–shell $NaYF_4$:Yb,Tm@TiO_2 upconversion microrods. Anal. Chem. 90, 1021–1028. https://doi.org/10.1021/acs.analchem.7b04479.

Salmonella Homepage, CDC [WWW Document], n.d. URL 〈https://www.cdc.gov/salmonella/index.html〉. (Accessed 5 January 2018).

Sayad, A.A., Ibrahim, F., Uddin, S.M., Pei, K.X., Mohktar, M.S., Madou, M., Thong, K.L., 2016. A microfluidic lab-on-a-disc integrated loop mediated isothermal amplification for foodborne pathogen detection. Sens. Actuators B Chem. 227, 600–609. https://doi.org/10.1016/J.SNB.2015.10.116.

Scallan, E., Hoekstra, R.M., Angulo, F.J., Tauxe, R.V., Widdowson, M.-A., Roy, S.L., Jones, J.L., Griffin, P.M., 2011. Foodborne illness acquired in the United States—major pathogens. Emerg. Infect. Dis. 17, 7–15. https://doi.org/10.3201/eid1701.P11101.

Singh, A., Poshtiban, S., Evoy, S., 2013. Recent advances in bacteriophage based biosensors for food-borne pathogen detection. Sensors 13, 1763–1786. https://doi.org/10.3390/s130201763.

Tokel, O., Yildiz, U.H., Inci, F., Durmus, N.G., Ekiz, O.O., Turker, B., Cetin, C., Rao, S., Sridhar, K., Natarajan, N., Shafiee, H., Dana, A., Demirci, U., 2015. Portable microfluidic integrated plasmonic platform for pathogen detection. Sci. Rep. 5, 9152. https://doi.org/10.1038/srep09152.

Vaisocherová-Lísalová, H., Víšová, I., Ermini, M.L., Špringer, T., Song, X.C., Mrázek, J., Lamačová, J., Scott Lynn, N., Šedivák, P., Homola, J., 2016. Low-fouling surface plasmon resonance biosensor for multi-step detection of foodborne bacterial pathogens in complex food samples. Biosens. Bioelectron. 80, 84–90. https://doi.org/10.1016/J.BIOS.2016.01.040.

W Stimson - US Patent App. 12/737, 2011. 995, undefined, n.d. Compositions and Methods for the Rapid Growth and Detection of Microorganisms. Google Patents.

Xu, M., Wang, R., Li, Y., 2016. Rapid detection of Escherichia coli O157:H7 and Salmonella Typhimurium in foods using an electrochemical immunosensor based on screen-printed interdigitated microelectrode and immunomagnetic separation. Talanta 148, 200–208. https://doi.org/10.1016/J.TALANTA.2015.10.082.

Yoo, S.M., Lee, S.Y., 2016. Optical biosensors for the detection of pathogenic microorganisms. Trends Biotechnol. 34, 7–25. https://doi.org/10.1016/J.TIBTECH.2015.09.012.

Zang, F., Gerasopoulos, K., Fan, X.Z., Brown, A.D., Culver, J.N., Ghodssi, R., 2016. Real-time monitoring of macromolecular biosensing probe self-assembly and on-chip ELISA using impedimetric microsensors. Biosens. Bioelectron. 81, 401–407. https://doi.org/10.1016/J.BIOS.2016.03.019.

Zeeshan, Daya, K.S, Tirumalai, P.S., Alocilja, E., 2018. Impedance and magnetohydrodynamic measurements for label free detection and differentiation of E. coli and S. aureus using magnetic nanoparticles. IEEE Trans. Nanobiosci. https://doi.org/10.1109/TNB.2018.2865384. (1–1).

Zheng, Q., Mikš-Krajnik, M., Yang, Y., Lee, S.-M., Lee, S.-C., Yuk, H.-G., 2016. Evaluation of real-time PCR coupled with immunomagnetic separation or centrifugation for the detection of healthy and sanitizer-injured Salmonella spp. on mung bean sprouts. Int. J. Food Microbiol. 222, 48–55. https://doi.org/10.1016/j.ijfoodmicro.2016.01.013.

Zhou, Q., Lin, Y., Zhang, K., Li, M., Tang, D., 2018. Reduced graphene oxide/BiFeO3 nanohybrids-based signal-on photoelectrochemical sensing system for prostate-specific antigen detection coupling with magnetic microfluidic device. Biosens. Bioelectron. 101, 146–152. https://doi.org/10.1016/J.BIOS.2017.10.027.